ASTM INTERNATIONAL

Materials Performance and Characterization

Stefano Beretta,[1] Michele Carboni,[2] and Daniele Regazzi[1]

DOI: 10.1520/MPC20140033

Load Interaction Effects in a Medium Strength Steel for Railway Axles

VOL. 4 / NO. 2 / 2015

Materials Performance and Characterization

doi:10.1520/MPC20140033 / Vol. 4 / No. 2 / 2015 / available online at www.astm.org

Stefano Beretta,[1] Michele Carboni,[2] and Daniele Regazzi[1]

Load Interaction Effects in a Medium Strength Steel for Railway Axles

Reference

Beretta, Stefano, Carboni, Michele, and Regazzi, Daniele, "Load Interaction Effects in a Medium Strength Steel for Railway Axles," *Materials Performance and Characterization*, Vol. 4, No. 2, 2015, pp. 168–181, doi:10.1520/MPC20140033. ISSN 2165-3992

ABSTRACT

As is well known, an interaction effect arises on crack propagation when a specimen or a component is subjected to variable amplitude fatigue loading. Depending on the applied load sequence, a certain amount of retardation or acceleration can then be observed, on the fatigue crack growth rate, with respect to the constant amplitude case. In the case of structural ductile materials, the interaction phenomenon is mainly addressed by the local plasticity at the crack tip and can be explained, from a global point of view, by adopting the crack closure concept. From this point of view, in the present research, load interaction effects in a medium strength steel for railway axles are analyzed. An experimental campaign was carried on this material, using SE(T) specimens, in order to understand and quantify the interaction effects arising from relevant load sequences derived from service. The experimental outcomes were then modeled adopting both a simple no-interaction approach and a more sophisticated strip-yield model in order to quantify the possible interaction effects. The modeling was carried out considering different experimental techniques for deriving the crack growth and threshold behaviors of the material, i.e., the traditional ΔK-decreasing technique and the compression pre-cracking one.

Keywords

crack propagation, variable amplitude loading, EA4T steel, compression pre-cracking, railway axles

Manuscript received March 2, 2014; accepted for publication August 14, 2014; published online September 26, 2014.

[1] Department of Mechanical Engineering, Politecnico di Milano, Via La Masa 1, 20156 Milano, Italy.

[2] Department of Mechanical Engineering, Politecnico di Milano, Via La Masa 1, 20156 Milano, Italy (Corresponding author), e-mail: michele.carboni@polimi.it

Introduction

Railway axles are usually designed against fatigue limit [1,2], but, due to their very long service life (30 years or even more on European lines) and to in-service damage like corrosion or ballast impacts, the approach has moved to damage tolerance [3–5]. From this point of view, the presence of cracks in axles is accepted and they must be periodically inspected using non-destructive techniques. The problem so moves to the determination of appropriate maintenance inspection intervals based on crack growth life predictions and the adopted non-destructive testing technique [6].

Considering the former aspect of inspection intervals, it is well known from the literature that an interaction effect on crack propagation arises when a specimen or a component is subjected to variable amplitude (VA) fatigue loading, like railway axles. Depending on the applied load sequence, a certain amount of retardation or acceleration in fatigue crack growth rate can then be observed if compared to the constant amplitude (CA) case. In the case of structural ductile materials, this interaction phenomenon is mainly addressed by the local plasticity at the crack tip and can be explained, from a global point of view, by adopting the "plasticity-induced crack closure" concept [7,8]. For example, a good correlation between crack growth interaction effects under variable amplitude loading and the amount of plasticity-induced crack closure has been previously derived by the authors [9], relatively to the standardized European EA1N steel (a normalized C40 grade) for railway axles [10].

A second critical aspect of crack growth predictions deals with the proper experimental procedure for generating threshold stress intensity factor (SIF) ranges. In particular, the traditional procedures are reported in the ASTM E647-05 standard [11] and are known as "ΔK-decreasing" and "constant K_{max}". Such procedures have been challenged [12,13] because it seems they influence the experimental results they generate. In order to fix these problems mainly related to the application of a load reduction technique, a different experimental procedure [12] is being increasingly adopted. It is based first on the pre-cracking of fracture mechanics specimens under cyclic compression [14], then on a stabilization step of crack growth. Finally, specimens are tested adopting proper load programs able to generate threshold values in conditions where load interaction effects are minimized due to the applied pre-cracking procedure. Such proper load programs are: (i) "compression pre-cracking constant amplitude" (CPCA), and (ii) "compression pre-cracking load reduction" (CPLR), where the load reduction technique is carried out so to minimize the interaction effects. In order to check which is the correct experimental approach for the EA1N steel, the authors compared (**Fig. 1**, [15]) the ΔK_{th} data generated using different procedures [15,16] with the results obtained from fatigue limit experiments on small defects and arranged in terms of the so called "Kitagawa–Takahashi" diagram (derived in Ref. [17] for the EA1N steel). As can be clearly seen, the correct estimation of the crack growth threshold seems to be, at least for the considered steel, the threshold SIF range obtained by compression pre-cracking techniques.

Another important topic regards the capability of traditional small-scale fracture mechanics specimens to describe crack propagation in full-scale axles. In addition, this subject has been studied by the authors, who defined [18] a modified thick version of the SE(T) specimen characterized by the same constraint found at the crack

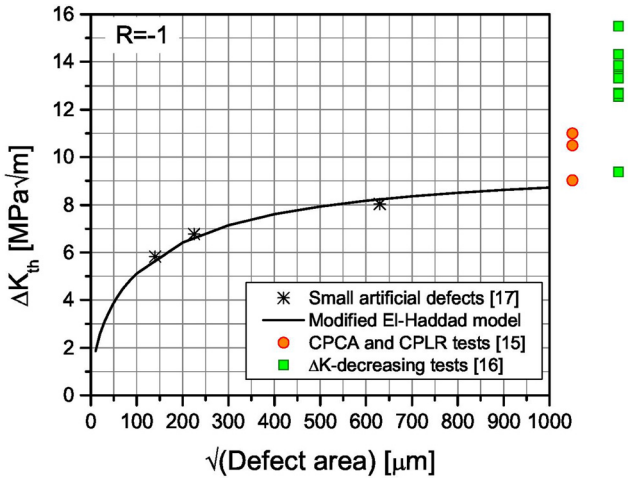

FIG. 1
Thresholds obtained by different techniques for the EA1N steel grade.

tip in axles and, consequently, able to compensate for the scale effect and to provide the same crack growth curves. Indeed, such a modified SE(T) specimen can be adopted as a "companion specimen" for full-scale axles.

The present paper deals with the other standardized European steel for railway axles: the medium strength EA4T [10], a quenched and tempered 25CrMo4 grade. Two batches of this steel grade were adopted, named, respectively, "batch A" and "batch B." Firstly, a CA loading experimental campaign, applying CPLR and CPCA experimental methodologies was carried out on EA4T batch B, using traditional small-scale SE(B) specimens, to compare the obtained data to existing ΔK-decreasing results [19] and to calibrate the parameters of Forman–Mettu equations [20]. Then, VA tests were performed on SE(T) companion specimens from the two batches. Crack propagation was experimentally measured considering the original in-service load time history and different equivalent block load sequences defined from it. This kind of analysis is particularly useful because the typical fatigue benches used for testing full-scale axles are not able to apply complex load time histories, but only block load sequences and the impact of this simplification should be known. In addition, a mean stress was eventually superimposed to the block load sequence in order to simulate the presence of a wheel press-fitted onto the railway axle and the consequent variation of the applied stress ratio from the typical $R = -1$ to higher values. Moreover, during each test, the crack closure at the crack tip was also experimentally measured. Crack growth predictions, using both a simple no-interaction algorithm and a more sophisticated strip–yield model [21], were finally carried out and compared to the experimental evidence.

Characterization of the Crack Propagation Behavior of EA4T Steel

A dedicated experimental campaign was carried out for each batch in order to investigate the crack propagation behavior of the EA4T grade at constant amplitude

loading. The near-threshold region was particularly investigated because, typically, the life of a railway axle is mostly spent within such a region.

Eight traditional SE(B) specimens from batch A and twelve from batch B, having a 12 by 24 mm^2 cross section and an 8 mm initial notch length obtained by electro-discharge machining (EDM), were tested. Each specimen was pre-cracked under compression adopting a mono-axial servo-hydraulic facility (maximum load equal to 100 kN) equipped with a dedicated four point bending device. In order to obtain a non-propagating and naturally arrested fatigue crack characterized by no closure effects, 200 000 cycles at bending moment $\Delta M = 160$ Nm, stress ratio $R = 10$ and 30 Hz were needed. The final length of pre-cracks resulted to be about 0.3 mm.

Crack propagation tests onto SE(B) specimens were then carried out using a Rumul Craktronic resonant plane bending facility having a capacity equal to 160 Nm and working at a frequency of about 130 Hz. Crack length was measured on either side of the crack, using 10 mm crack-gages and a dedicated central unit, by the potential drop technique. The specimens were tested at different stress ratios ranging from $R = 0.7$ to $R = -2.5$. At each considered stress ratio, both the crack growth rate and the threshold SIF range were investigated, by means of the CPCA and the CPLR techniques, respectively. At the end of the CPLR tests for threshold determination, if enough material remained, a CPCA test was carried out in order to complete the $da/dN - \Delta K$ diagram. ΔK-decreasing data, for batch B only, were instead previously derived and are already available in the literature [15].

Figure 2(*a*) shows the experimental crack growth curves obtained from each batch, along with their interpolation carried out applying the maximum likelihood method to the Forman–Mettu equation for crack growth rates [20]:

$$\frac{da}{dN} = C\left[\left(\frac{1-f}{1-R}\right)\Delta K\right]^{n} \frac{\left(1-\frac{\Delta K_{th}}{\Delta K}\right)^{p}}{\left(1-\frac{K_{\max}}{K_{crit}}\right)^{q}} \tag{1}$$

where:

C, n, p, and q = the empirical constants,

ΔK_{th} = the threshold SIF range,

FIG. 2 Constant amplitude crack growth characterization of the considered EA4T steel: (*a*) crack growth curves; (*b*) trend of thresholds with R.

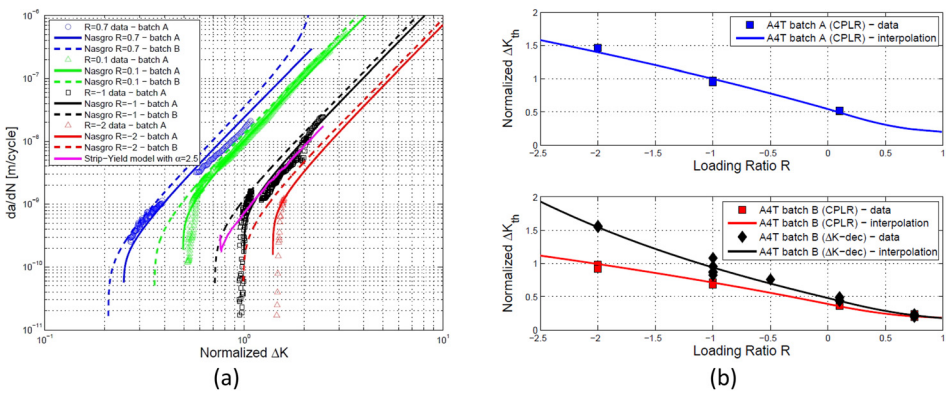

$K_{\max}$ and K_{crit} = the maximum and the critical SIF values, respectively,

R = the stress ratio, and

$f = S_{op}/S_{max}$ = the "Newman's closure function" [22] describing the plasticity-induced crack closure phenomenon.

Data were normalized due to their proprietary nature. In spite of the big differences, between the experimental approaches considered in the threshold region, the two data sets, from the two experimental methodologies for batch B steel grade, are in good agreement in the linear region of the $da/dN - \Delta K$ diagram, as was shown by the authors [19].

Figure 2(*b*) shows (normalized again), then, the trend of thresholds with stress ratio R, as derived from the current experimental campaigns, and compares it to data available in the literature [15] and obtained by the ΔK-decreasing technique (batch B only). The figure also shows the interpolation of experimental data, applying again the maximum likelihood method, by the Forman–Mettu equation for thresholds [20]:

$$\Delta K_{th} = \Delta K_o \cdot \sqrt{\frac{a}{a + a_o}} \Big/ \left[\frac{1 - f}{(1 - A_o)(1 - R)}\right]^{(1+C_{th}R)} \tag{2}$$

where:

A_o = a constant in the formulation of f,

ΔK_0 = the threshold value at $R = 0$,

C_{th} = an empirical constant,

a = the crack length, and

a_o = the El-Haddad parameter [23].

The dependence of ΔK_{th} with R is controlled through the C_{th} parameter: different values of C_{th} (namely $C_{\text{th}+}$ and $C_{\text{th}-}$) have to be considered for positives and negatives R-values. It is worth noticing that Eq 2 is generally valid in the range $-2 \leq R \leq 0.7$: outside these limits, thresholds are usually considered constant. This behavior is here: (i) rather evident considering compression pre-cracking data, but not ΔK-decreasing results; (ii) supported by the observation that data obtained at $R = -2.5$ along the linear region superimpose very well with those obtained at $R = -2$. The empirical parameters determined by interpolating experimental data were then ΔK_0, $C_{\text{th}+}$, and $C_{\text{th}-}$: it is evident that the compression pre-cracking technique results in lower thresholds when compared to the traditional approach, especially considering the lowest stress ratios. This is in accordance to what was found for the EA1N steel [15]. The threshold trend line of EA4T batch A is higher over the whole stress ratio R range, as in **Fig. 2(*b*)**.

Since it was not possible to carry out threshold experiments on EA4T batch A steel grade adopting the $\Delta K-$decreasing methodology, the increase of ΔK_{th} at $R = -1$, for prospective crack growth simulations adopting the threshold trend from ΔK-decreasing, was estimated to be approximately 15 %, as for EA4T batch B data.

Variable Amplitude Loading Experiments

A new type [18] of SE(T) specimen (width equal to 50 mm and thickness equal to 20 mm, **Fig. 3(*a*)**), having the same crack tip "constraint" of cracks in real axles, was

FIG. 3 Experimental setup for variable amplitude loading tests: (*a*) geometry of the adopted SE(T) specimen; (*b*) example of generated non-propagating and closure-free crack after "razor sliding" and compression pre-cracking: final length equal to 0.096 mm; (*c*) detail of a specimen instrumented by crack-gages, clip-gage and strain-gages.

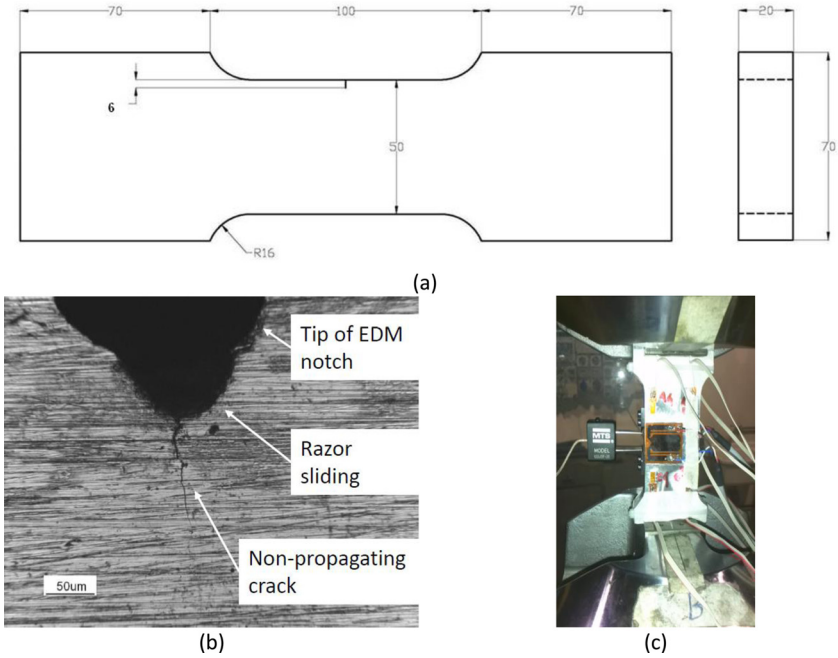

adopted for the variable amplitude loading experiments as companion specimen for full-scale axles. The initial notch, 6 mm deep and obtained by EDM, was extended by sliding a razor blade into the material. By this technique, it was possible to get extremely sharp notches: the sharper the notch, the smaller the load to initiate a pre-crack at the notch root and the smaller the required length of the pre-crack to eliminate notch effects. Tests were then performed by a mono-axial servo-hydraulic Schenck facility with 250 kN maximum load. First, the specimens were pre-cracked under compression in order to obtain, similar to the small-scale SE(B) specimens, a non-propagating and naturally arrested fatigue crack characterized by no closure effects. About 200 000 cycles at $\Delta F = 124$ kN, $R = 10$ and 20 Hz were needed for this purpose. The final length of all pre-cracks was documented by optical microscopy and resulted to be about 0.1 mm (**Fig. 3(*b*)** shows an example).

After compression pre-cracking, each specimen was instrumented by two 20 mm crack-gages, one on either side, for the real-time crack length monitoring by a potential drop technique. A clip-gage, located across the crack mouth, and the "compliance offset" methodology described in ASTM E647 [11] allowed performing the evaluation of crack closure. Moreover, before starting each test, eight strain gages were glued on each specimen, as visible in **Fig. 3(*c*)**, in order to verify the correct alignment of the load axis.

Experimental crack growth data obtained from each test were post-processed by the secant method [11] and the applied SIF range was calculated using Eq 3, which was obtained by a finite element analysis during previous activities [18]:

$$\Delta K = \left[\Delta\sigma \cdot \left(3.15 \cdot 10^{-4} \cdot a^2 + 3.63 \cdot 10^{-3} \cdot a + 1.09\right) \cdot \sqrt{\pi \cdot a/1000}\right] \quad (3)$$

where:
ΔK is in (MPa$\sqrt{}$m),
$\Delta\sigma$ is the applied axial stress range (MPa), and "a" is the measured crack length (expressed in millimeter).

The finite element analysis was required for the adopted specimen, characterized by constrained ends, because it is not included in the ASTM E647 standard [11].

The first two SE(T) specimens (EA4T batch B steel grade) were tested (**Table 1**) with the aim to check the crack propagation behavior of the material subjected to a load-time history and to an equivalent block load sequence derived from the time history itself. These experiments were also performed because the typical fatigue benches used for testing full-scale axles are not able to apply load time histories, but only block load sequences and the possible differences in the response could be checked. The applied load-time history is representative of 57 000 km of service and was derived by in-line measurements onto a high-speed train. **Figure 4(*a*)** shows the load spectrum of the load-time history and compares it to its equivalent block loads: the blocks were rearranged according to a Gassner sequence [24] typically adopted by some European railway operators for the homologation of axles and defined as "long blocks" (**Fig. 4(*b*)**). The amplitudes of both the load-time history and the block load sequence were applied to specimens after being scaled so that their maximum ΔK_{max} at the beginning of each test was the same of the one at the tip of a 2.5 mm deep crack located in the most stressed section along the groove of a real axle.

Figure 5(*a*) directly compares the crack advance Δa registered during the two tests. As can be seen, they seem comparable, at least over the initial propagation of the crack. It is also worth adding that such crack advance was considered for both tests starting from the stabilization of the closure level, as shown in **Figs. 5(*b*)** and **5(*c*)**. In particular, after the stabilization, the experimental $U = \Delta K_{eff}/\Delta K$ value resulted to be about 0.35 for both tests, in accordance with the indications given by Schijve [25] for $R = -1$.

Regarding the tests onto EA4T batch A steel grade, the load spectrum was amplified, compared to specimens from batch B, by 25 %, and the mean stress of **Fig. 4(*a*)** was also considered. This mean stress value was added to each block of the load spectrum, then rearranged in the already adopted Gassner sequence, obtaining the block load sequence shown, again normalized, in **Fig. 4(*b*)**. It is worth noticing that, due to the superposition of the constant stress value onto the load spectrum, the resulting stress ratio moves from the typical value $R = -1$ (just rotating bending), to less negative values. The acting stress ratios are between zero and minus one.

TABLE 1

Summary of the VA experiments carried out.

Specimen	Steel Grade	VA Loading	$S_{max}/S_{y\ cyc}$	$\Delta K_{max}/\Delta K_{th}$
A4T-SE(T)#1	EA4T batch A	Long blocks ($R \neq -1$)	0.21	2.0
A4T-SE(T)#2	EA4T batch A	Short blocks ($R \neq -1$)	0.21	2.0
A4T2-SE(T)#4	EA4T batch B	Time history ($R = -1$)	0.20	1.2
A4T2-SE(T)#5	EA4T batch B	Long blocks ($R = -1$)	0.20	1.2

FIG. 4 Normalized VA loadings derived from in-line service: (*a*) equivalent block load spectrum (R = −1); (*b*) adopted Gassner block load sequences (R ≠ −1): long blocks (upper figure) against short blocks (lower figure).

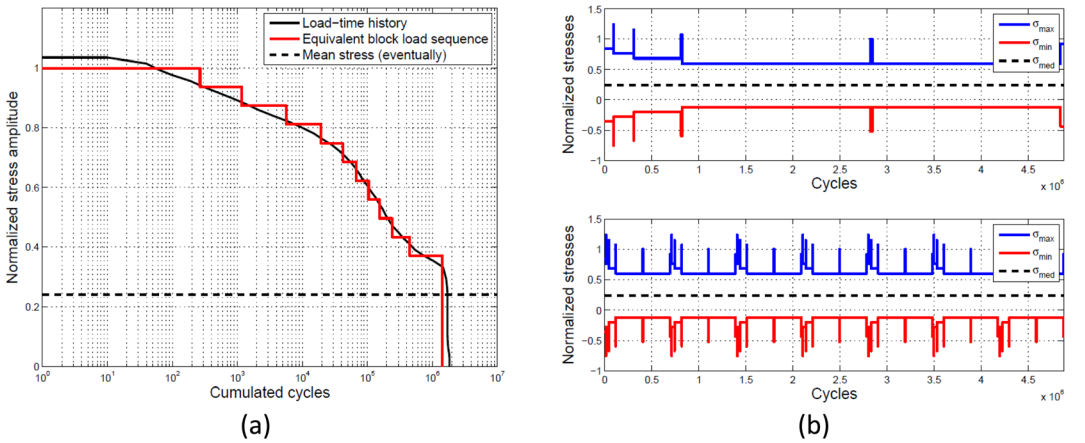

Since the aim of this research was to understand the effect of the block length onto crack propagation, two different block's lengths were adopted: the "longer" one (upper plot in **Fig. 4(*b*)**), composed of about 5×10^6 cycles, and a "shorter" one, obtained dividing the number of cycles of each block of the longer one by seven (lower plot in **Fig. 4(*b*)**). Specimen A4T-SE(T)#1 was tested applying the longer block sequence, while specimen A4T-SE(T)#2 was tested using the shorter one.

Results of crack propagation on the two tested specimens, both from batch A, are shown in **Fig. 6(*a*)**. As can be seen, both experiments lasted about 25×10^6 cycles and crack propagation curves match very well. As for EA4T batch B steel grade, there is no additional interaction effect due to the length of the blocks for the considered material.

The U ratio, recorded during the tests, is shown in **Figs. 6(*b*)** and **6(*c*)**. As can be seen, it is higher than expected: the two red dotted lines, representing the extreme values according to Schijve's formulation [25] at the involved stress ratios, are lower than the experimental outcomes, which, anyway, showed comparable trends. This behavior appears to be due to the fact that at the lower stress amplitudes (when crack advance is negligible), S_{op} values remain "frozen" at the values of the higher stress amplitudes, where a sudden crack advance happens. This higher U ratio should indicate a faster crack growth, while, in reality, the crack does not propagate at all during the lower load levels, because of the crack tip plasticity induced by the higher ones.

Crack Growth Simulations

Crack growth simulations were initially carried out using a simple no-interaction model, adopting both CPLR and ΔK-decreasing thresholds, in order to quantify how much the experimental methodology for the definition of the thresholds can affect the predictions. Then, a more refined attempt to match lifetime predictions to the experiments consisted in the use of the more sophisticated strip–yield model, as implemented in the commercial software Nasgro [26]. By the strip–yield model, it is possible to take into account for interaction effects during propagation due to crack tip plasticity and the consequent crack closure. The experimental effective crack

FIG. 5 Experimental results of the tests carried out onto EA4T batch B specimens: (*a*) comparison of crack propagation applying time history or equivalent block loading; (*b*) crack closure measurements during the load-time history test; (*c*) crack closure measurements during the equivalent block load sequence test.

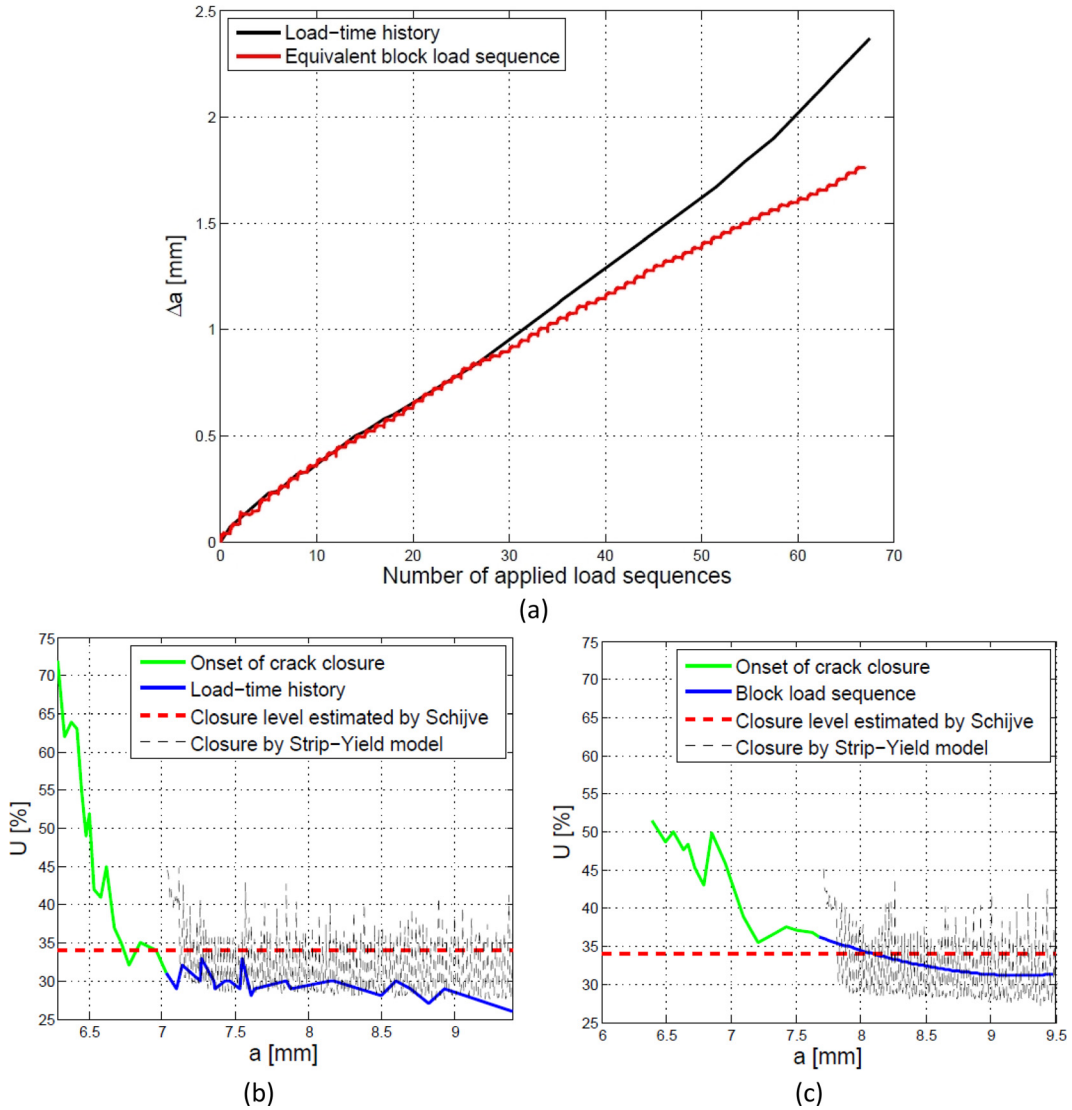

growth curve (conventionally taken at $R = 0.7$) of each batch of EA4T steel grade, derived from the CPLR experimental methodology, was provided as input for material calculations, as in **Fig. 2(*a*)**.

The constraint factor values for strip yield simulations were set for both batches at $\alpha = 2.5$ according to Nasgro's user manual [26]. This assumption was first verified by CA crack growth simulations at stress ratio $R = -1$, returning in a good description of crack growth curves onto SE(T) specimens [27]. As shown in **Fig. 2(*a*)**, simulations by the strip–yield model calibrated using $\alpha = 2.5$ are very close to the Nasgro fitting at the stress ratio $R = -1$, confirming the validity of the chosen α value.

FIG. 6 Experimental results of the tests carried out onto EA4T batch A specimens: (*a*) comparison of crack propagation applying long and short blocks; (*b*) crack closure measurements during the test with long block sequence; (*c*) crack closure measurements during the test with short block sequence.

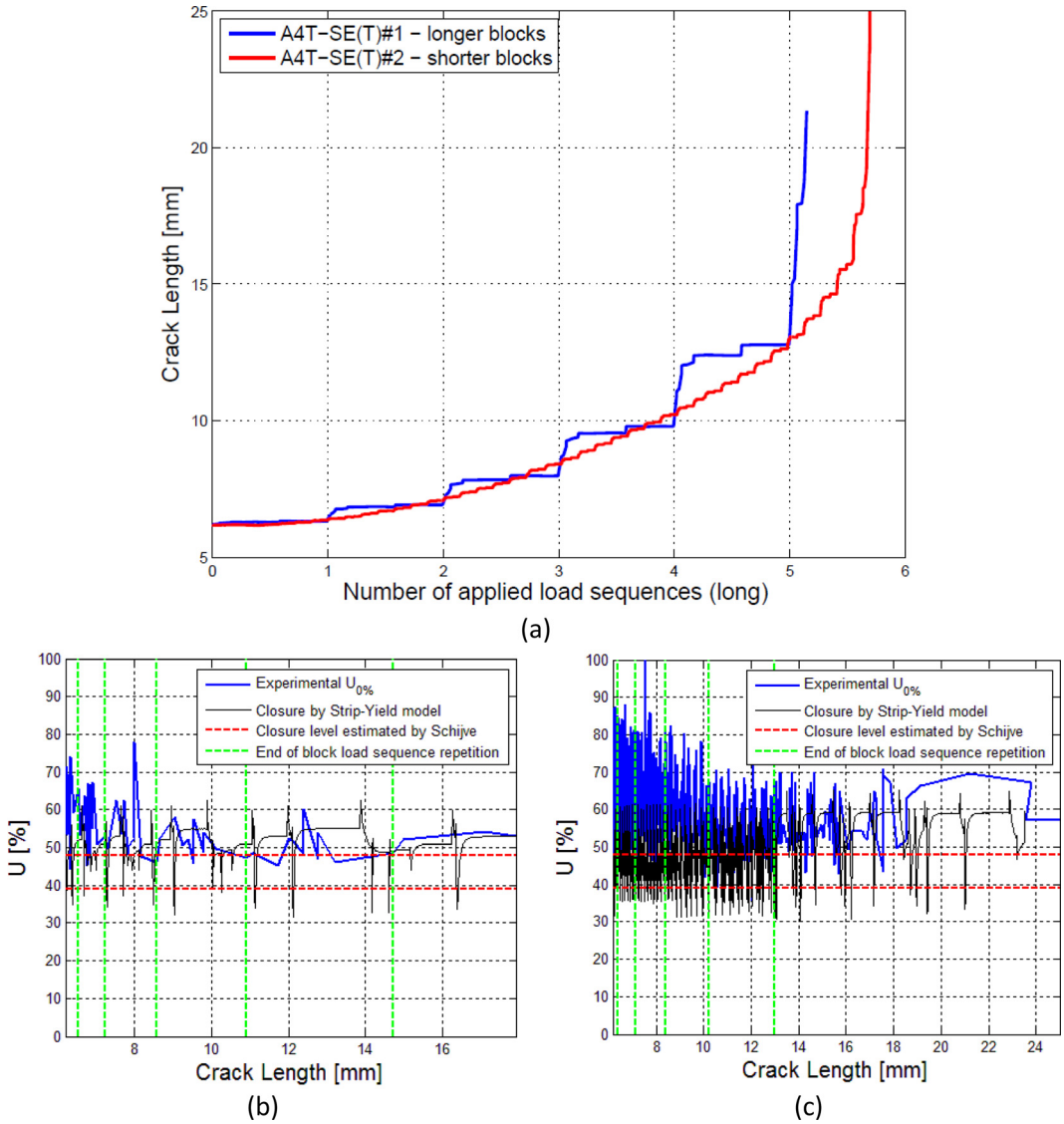

A first result, clearly appearing in **Figs. 7** and **8**, is that, for all the tested specimens, the experiments always lie in between the no-interaction simulations performed by CPLR and ΔK-decreasing methodologies. In particular, adopting the CPLR parameters, the simulations always result in conservative predictions, while, on the contrary, they result in non-conservative predictions when adopting the ΔK-decreasing parameters. This is true for both the EA4T batches and for each shape of the applied loading program.

Regarding the simulations by the strip–yield model, a value of α close to 3 was suggested [28] for the modified SE(T) specimens made of EA1N, but the evidence

FIG. 7 Crack growth simulations, by no-interaction and strip–yield models, of the tests carried out onto EA4T batch B specimens: (*a*) specimen A4T2-SE(T)#4; (*b*) specimen A4T2-SE(T)#5.

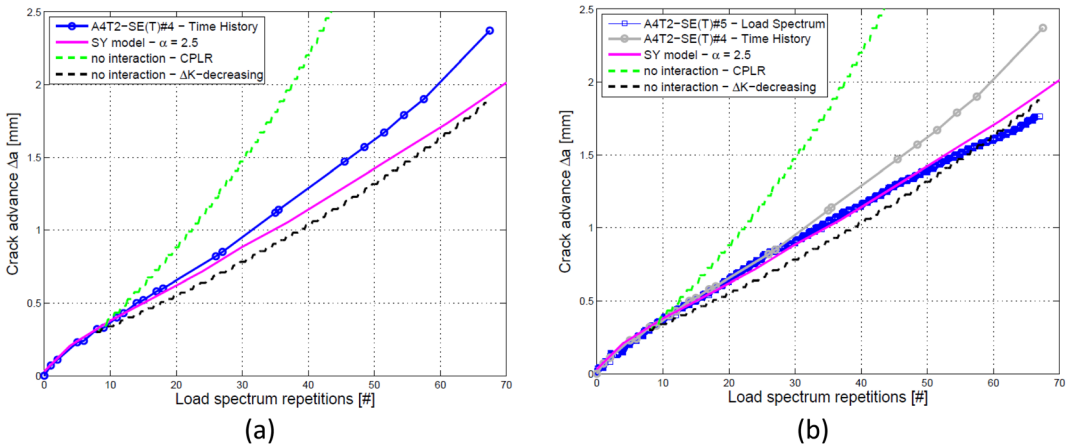

for the EA4T steel grade here is in contradictions with this indication, as was shown for the constant amplitude strip–yield simulations at $R = -1$ (**Fig. 2(*a*)**). A constraint factor value close to 2.5 was found to be adequate, as stated above, for crack growth predictions of both EA4T batches; thus remaining on the safe side, as in **Figs. 7** and **8**. The evidence, regarding the tests under variable amplitude loading, is that a slight retardation appears due to the interaction between load levels, and this can be well represented by the strip–yield model. This is also supported by the estimated numerical values of closure (**Figs. 5** and **6**), which present a trend reasonably comparable to the experimental ones for all the considered variable amplitude tests. Anyway, it is worth remarking that the amount of retardation does not rely to the shape of the applied load sequence.

FIG. 8 Crack growth simulations, by no-interaction and strip–yield models, of the tests carried out onto EA4T batch A specimens: (*a*) Specimen A4T-SE(T)#1; (*b*) Specimen A4T-SE(T)#2.

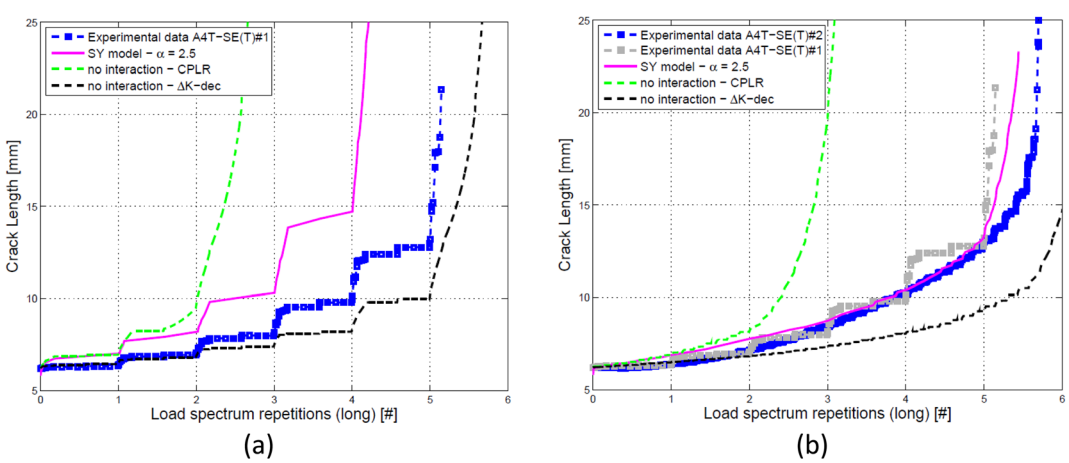

Concluding Remarks

The effect of variable amplitude loading on crack propagation was considered, relatively to two batches of the medium strength steel 25CrMo4 (commercial grade EA4T), typically adopted in the railway axles production. The results of the research can be summarized:

- The two bathes of EA4T material resulted in different thresholds, with batch A showing results higher (up to $10 \div 15$ %) than batch B, while the linear portion of the Paris diagrams are nearly identical;
- Thresholds obtained by CPLR and ΔK-decreasing methodologies resulted to be quite different for the EA4T batch B grade, with CPLR being lower, of about 15 %, at stress ratio $R = -1$;
- No evidence of an interaction effect arose in terms of the shape of the applied VA loading, for both batches: results derived applying a load–time history versus an equivalent block load sequence, or long blocks versus short ones, are always in good agreement; this allows the application of load sequences to full-scale specimens (where it is not feasible to apply a load–time history) without affecting the results;
- Measurements of crack closure under VA conditions, via the U ratio, were found to be always higher than expected; this behavior appears to be related to the fact that almost no propagation happened at lower load levels. The crack closure remained "frozen" at high levels, not having sufficient crack advance to stabilize;
- The experimental evidence is always in between the no-interaction simulations considering thresholds from CPLR (conservative predictions) and ΔK-decreasing (non-conservative predictions);
- An evident retardation effect clearly appears with respect to no-interaction predictions adopting CPLR thresholds; such a retardation effect was justified and quantified by the performed strip yield simulations.

References

[1] EN 13103: Railway Applications—Wheelset and Bogies—Non-Powered Axles—Design Method, European Committee for Standardization, Technical Committee CEN/TC 25, Paris, France, 2012.

[2] EN 13104: Railway Applications—Wheelset and Bogies—Powered Axles—Design Method, European Committee for Standardization, Technical Committee CEN/TC 25, Paris, France, 2012.

[3] Grandt, A. F., Jr., *Fundamentals of Structural Integrity*, John Wiley & Sons, New York, 2004.

[4] Zerbst, U., Lunden, R., Edel, K.-O., and Smith, R. A., "Introduction to the Damage Tolerance Behavior of Railway Rails—A Review," *Eng. Fract. Mech.*, Vol. 76, No. 17, 2009, pp. 2563–2601.

[5] Cantini, S. and Beretta S., Eds., Structural Reliability Assessment of Railway Axles, LRS–Techno Series, Lovere, Italy, 2011.

[6] Cantini, S., Beretta, S., and Carboni, M., "POD and Inspection Intervals of High Speed Railway Axles," *Proceedings of the 15th International Wheelset Congress*, Prague, Czech Republic, Sept 23–27, 2007.

[7] Schijve, J., *Fatigue Crack Propagation in Light Alloy Sheet Materials and Structures*, Vol. 3, *Pergamon Press*, 1961.

[8] Handrock, J. L., Bannantine, J. A., and Comer, J. J., *Fundamentals of Metal Fatigue Analysis*, Prentice Hall, Upper Saddle River, NJ. 1990.

[9] Beretta, S. and Carboni, M., "Variable Amplitude Fatigue Crack Growth in a Mild Steel for Railway Axles: Experiments and Predictive Models," *Eng. Fract. Mech.*, Vol. 78, 2011, pp. 848–862.

[10] EN 13261: Railway Application—Wheelsets and Bogies—Axles—Product Requirements, European Committee for Standardization, Technical Committee CEN/TC 25, Paris, France, 2011.

[11] ASTM E647-05: Standard Test Method for Measurement of Fatigue Crack Growth Rates, *Annual Book of ASTM Standards*, ASTM International, West Conshohocken, PA, 2005.

[12] Pippan, R., Stüwe, H. P. and Golos, K., "A Comparison of Different Methods to Determine the Threshold of Fatigue Crack Propagation," *Fatigue*, Vol. 16, No. 8, 1994, pp. 579–582.

[13] Forth, S. C., Newman, J. Jr., and Forman, R. G., "On Generating Fatigue Crack Growth Thresholds," *Int. J. Fatigue*, Vol. 25, No. 1, 2003, pp. 9–15.

[14] Pippan, R., "The Growth of Short Cracks Under Cyclic Compression," *Fatigue Fract. Eng. Mater. Struct.*, Vol. 9, No. 5, 1987, pp. 319–328.

[15] Carboni, M., Patriarca, L., and Regazzi, D., "Determination of ΔK_{th} by Compression Pre-Cracking in a Structural Steel," *J. ASTM Int.*, Vol. 6, 2009, pp. 1–13.

[16] Beretta, S., Carboni, M., Cantini, S., and Ghidini, A., "Application of Fatigue Crack Growth Algorithms to Railway Axles and Comparison of Two Steel Grades," *J. Rail Rapid Transit*, Vol. 218, No. 4, 2004, pp. 317–326.

[17] Beretta, S., Carboni, M., Lo Conte, A., and Palermo, E., "An Investigation of the Effects of Corrosion on the Fatigue Strength of A1N Axle Steel," *J. Rail Rapid Transit*, Vol. 222, 2008, pp. 129–143.

[18] Carboni, M., Beretta, S., and Madia, M., "Analysis of Crack Growth at $R = -1$ Under Variable Amplitude Loading on a Steel for Railway Axles," *J. ASTM Int.*, Vol. 5, No. 7, 2008, pp. 1–13.

[19] Carboni, M. and Regazzi, D., "Effect of the Experimental Technique onto R Dependence of Kth," *Proc. Eng.* Vol. 10, 2011, pp. 2937–2942.

[20] Forman, R. G. and Mettu, S. R., "Behavior of Surface and Corner Cracks Subjected to Tensile and Bending Loads in Ti-6Al-4V Alloy," *Fracture Mechanics: Twenty-Second Symposium, ASTM STP 1131*, ASTM International, West Conshohocken, PA, 1992, pp. 948–953.

[21] Newman, J. C., Jr., "A Crack–Closure Model for Predicting Fatigue Crack Growth Under Aircraft Spectrum Loading," *ASTM STP* 748, ASTM International, Philadelphia, PA, 1981, pp. 53–84.

[22] Newman, J., Jr., "A Crack Opening Stress Equation for Fatigue Crack Growth," *Int. J. Fract.*, Vol. 24, No. 4, 1984, pp. R131–R135.

[23] El–Haddad, M. H., Smith, K. N., and Topper, T. H., "Fatigue Crack Propagation of Short Cracks," *ASME Trans. J. Eng. Mater. Technol.*, Vol. 101, No. 1, 1979, pp. 42–46.

[24] Gaßner, E., *Auswirkung BetriebšAhnlicher Belastungsfolgen auf die Festigkeit von Flugzeugbauteilen*, Jahrbuch Deutsch, Luftfahrtforschung, Germany, 1941, pp. 472–483.

[25] Schijve, J., "Some Formulas for the Crack Opening Stress Level," *Eng. Fract. Mech.*, Vol. 14, No. 3, 1981, pp. 461–465.

[26] Nasgro, N. J. S. C., *Fatigue Crack Growth Computer Program Nasgro Version 4.2–Reference Manual*, SRI, San Antonio, TX, 2006.

[27] Regazzi, D., 2014, "Advances in Life Prediction and Durability of Railway Axles," Ph.D. thesis, Politecnico di Milano, Milan, Italy.

[28] Carboni, M., Beretta, S. and Madia, M., "Analysis of Crack Growth at R = –1 Under Variable Amplitude Loading on a Steel for Railway Axles," *J. ASTM Int.*, Vol. 5, No. 7, 2008, 101648.